International Journal of Pharmaceutics, 62 (1990) 217–228
Elsevier

IJP 02105

Transparent oil-water gels.
Part II. A study of the gel structure in transparent oil-water gels by differential scanning calorimetry

C. Provost, H. Herbots and R. Kinget

Laboratorium voor Galenische en Klinische Farmacie, Katholieke Universiteit Leuven, Leuven (Belgium)

(Received 18 December 1989)
(Accepted 27 January 1990)

Key words: Transparent oil-water gel; Nonionic emulsifying agent; DSC; Gel structure; Differential scanning calorimetry

Summary

The elements controlling the formation of transparent oil-water gels in a four-component system were investigated by means of differential scanning calorimetry. The model system had two emulsifying agents, Cetiol^R HE and Eumulgin^R B3, an oily liquid, isopropyl palmitate, and water. The thermal behaviour of the single components and of some of their binary emulsifier-water and ternary emulsifier-oil-water mixtures was also studied. The results showed that the mechanism underlying the formation of transparent oil-water gels involved an interaction of isopropyl palmitate with one or both hydrated emulsifiers. Not only the behaviour of the emulsifiers in water but also the melting behaviour of isopropyl palmitate and the melting of the gel were clearly affected by the oil content of the gel. An increase in structural organisation can be inferred from the evolution of the melting point of the gel with increasing isopropyl palmitate concentrations. The binding forces responsible for the gel structure seem to be hydrogen bonds.

Introduction

We use the term ‘transparent oil-water gels’ (TOW gels) (Provost, 1986) for semisolid systems that consist mainly of water, oil and hydrophilic emulsifier(s), and that are characterized by a jelly-like consistency, transparency, homogeneity, optical isotropy, thermodynamic stability and resonance when a containerful is tapped. In a previous paper, we examined the formation of TOW gels in a four-component model system. The quaternary system has two emulsifying agents, Cetiol^R HE (CHE) and Eumulgin^R B3 (EB3), an oily liquid, isopropyl palmitate (IPP), and water (H_2O). The phase diagram indicated that the presence of both the oil phase and the two emulsifiers is essential for their formation (Provost and Kinget, 1988a). Viscosity measurements showed that the concentration of the components plays an essential role in the gel structure (Provost et al., 1988b).

However, neither the mechanisms and intercomponent interactions underlying the gel formation nor the elements controlling the construction

---

Correspondence: C. Provost, Laboratorium voor Galenische en Klinische Farmacie, Katholieke Universiteit Leuven, Campus Gasthuisberg, Onderwijs en Navorsing, B-3000 Leuven, Belgium.

of the gel structure and its strength are fully understood. Fundamental investigations of the physico-chemical characteristics and the gel structure of TOW gels are rare. Little is known about their colloidal chemical structure.

Creams have been studied more extensively, and it has been shown that the colloidal structure of creams affects both the release of drugs (Boddé et al., 1986) and of water (Junginger et al., 1984). Therefore, a deeper understanding of the microstructure of TOW gels might well allow for the development of a formulation with controlled drug and water release. The interesting cosmetic, usage and technological qualities (Provost, 1986) of TOW gels as well as their biopharmaceutical characteristics with regard to both release (Provost et al., 1989a) and skin penetration (Provost et al., 1989b) of hydrophilic and lipophilic drugs should also be considered.

In the present paper, we determine some of the elements controlling the formation of the gel structure in our TOW gels by means of differential scanning calorimetry (DSC). First, the single components CHE, EB3, and IPP are investigated. Second, CHE-H_2O, EB3-H_2O, and CHE-EB3-H_2O mixtures are studied. These experiments supply information on the structural associations formed by the emulsifiers in water, the hydration of the emulsifiers (De Vringer et al., 1986a; Heusch, 1983), and possible interactions between CHE and EB3. IPP is then added to the binary emulsifier-water mixtures, which allows the influence of the oil phase to be examined. Finally, four TOW gels, each containing a different amount of IPP, are investigated. The gel character of the TOW gels is further studied by measuring their melting temperature as a function of their IPP content. The melting points of quaternary CHE-EB3-IPP-H_2O creams containing still higher IPP concentrations are compared.

Materials and Methods

Both of the emulsifying agents, Cetiol^R HE (Henkel & Cie, Düsseldorf) and Eumulgin^R B3 (Henkel & Cie, Düsseldorf) were used as supplied without further purification. Their chemical composition is represented in Figs 1 and 2, respectively. The isopropyl palmitate (U.S.N.F. XVI), demineralized water, and phenylmercuric nitrate (U.S.N.F. XVI) were of pharmacopoeial quality.

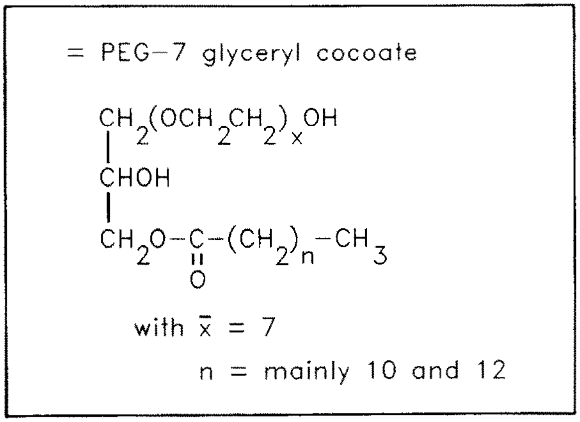
= PEG-7 glyceryl cocoate

$$\begin{array}{l} CH_2(OCH_2CH_2)_xOH \\ | \\ CHOH \\ | \\ CH_2O-\underset{\underset{O}{\|}}{C}-(CH_2)_n-CH_3 \end{array}$$

with $\bar{x} = 7$

n = mainly 10 and 12

Fig. 1. Schematic representation of the chemical composition of Cetiol^R HE.

Sample preparation and composition

The binary, ternary and quaternary mixtures were prepared as described elsewhere (Provost and Kinget, 1988a). The samples were stored at room temperature in air-tight glass containers for at least 1 week prior to their examination. Their exact composition was determined by means of a method described elsewhere (Provost and Kinget, 1988a).

Four series of compositions were investigated by means of DSC:

= Ceteareth-30

= PEG-ether of cetostearyl alcohol

$R(OCH_2CH_2)_nOH$

with R = blend of cetyl and stearyl radicals

$\bar{n} = 30$

Fig. 2. Schematic representation of the chemical composition of Eumulgin^R B3.

TABLE 1

Composition of the TOW gels under investigation

TOW gel	Composition (%w/w)			
	CHE	EB3	IPP	H_2O+PN
1	18	15	2	65
2	18	15	5	62
3	18	15	8	59
4	30	12	13	45

For abbreviations see text.

- the single components CHE, EB3 and IPP;
- emulsifier-water mixtures CHE-H_2O, EB3-H_2O and CHE-EB3-H_2O;
- ternary emulsifier-IPP-water mixtures, i.e., CHE-IPP-H_2O and EB3-IPP-H_2O; and
- four TOW gels each containing a different amount of IPP, the compositions of which are given in Table 1.

The composition of the binary and ternary mixtures was selected in such a way that their CHE, EB3, and IPP content, expressed as %w/w, corresponded to their concentration in the TOW gels under investigation.

In order to prevent microbial contamination, the water used for sample preparation contained 0.002% phenylmercuric nitrate (PN). All the samples were examined microscopically with normally transmitted and polarized light.

Differential scanning calorimetry

A Perkin-Elmer DSC-2C differential scanning calorimeter was used. The specimens, which weighed between 5 to 25 mg, depending on the nature of the material, were hermetically sealed in DSC cups in order to avoid water loss through evaporation. An empty hermetic cup was used as the reference. The samples were cooled from ambient temperatures to $-50\,^{\circ}C$ at a rate of $80\,^{\circ}C/min$. After equilibration, thermograms were obtained by heating the specimens up to $90\,^{\circ}C$, cooling them to $-50\,^{\circ}C$, and again heating them to $90\,^{\circ}C$, each time using a rate of $5\,^{\circ}C/min$. The enthalpy changes were obtained from the areas of the thermogram peaks by constructing a linear baseline from peak onset to completion and numerically integrating the enclosed area. The results are given in J/g. Unless otherwise specified, the transitions were further characterized by their onset temperature, which was defined as the temperature at which the leading edge of the peak intersects the baseline.

Determination of melting point

The melting points of the TOW gels and of some other semisolid quaternary CHE-EB3-IPP-H_2O mixtures were determined with an Ubbelohde Apparatus as described in the British Pharmacopoeia (1988). At least three measurements were made on each sample.

Results and Discussion

Single components

Cetiol^{R} HE

During heating and cooling of Cetiol^{R} HE, a single, very broad transition was observed. In the heating curve (Fig. 3), this endothermal transition extended from the lower part of the investigated temperature region to $0\,^{\circ}C$ and is due to the melting of the surfactant. The broadness of the melting process originates from the molecular weight distribution of this compound and the presence of impurities. In the cooling curve the corresponding exothermal effect showed a minimum at $-11.9\,^{\circ}C$.

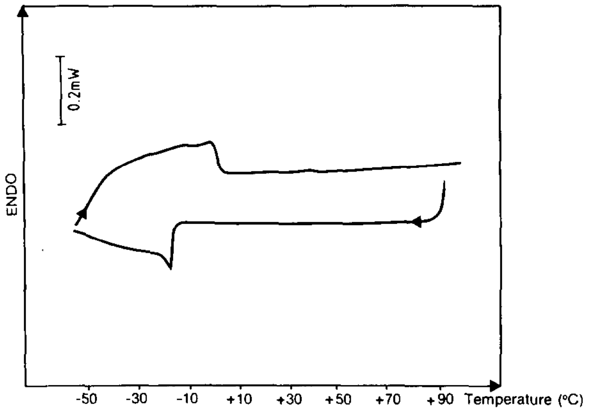

Fig. 3. Normalized DSC heating and cooling curves of Cetiol^{R} HE.

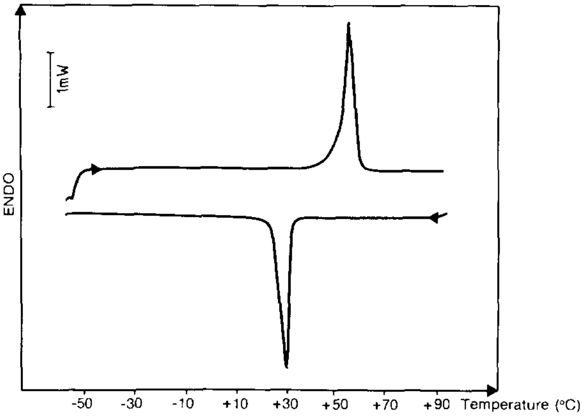

Fig. 4. Normalized DSC heating and cooling curves of Eumulgin^{R} B3.

Eumulgin^{R} B3

In the heat flow scan of Eumulgin^{R} B3 (Fig. 4), one peak was detected, showing an onset temperature of 51° C and a maximum at 55° C. The heat effect was endothermal and appeared when the crystalline surfactant melted to form an isotropic liquid. Upon cooling, because of the supercooling, recrystallization only started at 32° C, with a minimum at 28° C. Since Eumulgin^{R} B3 contains higher and lower homologues of the polyoxyethylene and the hydrocarbon chains and might have impurities, the melting occurred over a fairly broad temperature range. This effect, however, was less pronounced than for Cetiol^{R} HE.

In an investigation into the thermal behaviour of poly(oxyethylene)$_{20}$ glycerolmonostearate (PGM$_{20}$), de Vringer et al. (1986b) observed that the melting of this surfactant was composed of two separate phenomena: the melting of the polyoxyethylene domains and, at somewhat higher temperatures, the melting of the hydrocarbon chains. However, our findings for Eumulgin^{R} B3 concerning both melting point and melting enthalpy strongly suggest that the hydrophilic and the lipophilic chains melt simultaneously. Indeed, the onset temperature of the melting process, 51° C, agrees well with the value reported for the melting of commercially available cetostearyl alcohol (De Vringer et al., 1986b; Junginger et al., 1979a) as well as with the melting points of pure poly(ethylene glycol)s with similar molecular weights (Reynolds, 1982, De Vringer et al., 1986a; Fiedler, 1989). Since the melting of cetostearyl alcohol involves an enthalpy change of 128 J/g (De Vringer et al., 1986b), the melting of the hydrocarbon chains of Eumulgin^{R} B3, which represent approximately 16.5% (w/w) of its molecular weight, would take circa 21 J/g. From the melting enthalpy reported for normally available poly(ethylene glycol) 1500, i.e., 163.8 ± 0.6 J/g (Junginger et al., 1980) and from the heat of fusion of 100% crystalline polyoxyethylene (Flory, 1953), it can be calculated that melting of the oxyethylene chains in Eumulgin^{R} B3 would require approximately 137 to 160 J/g. Adding up these theoretical values for the melting enthalpies of the hydrocarbon chain and the polyoxyethylene chain yields a value of approximately 158 to 181 J/g, which is very close to the measured enthalpy of 168 J/g.

Isopropyl palmitate

The DSC graphs obtained for IPP (Fig. 5) showed several heat effects. The first two endo-

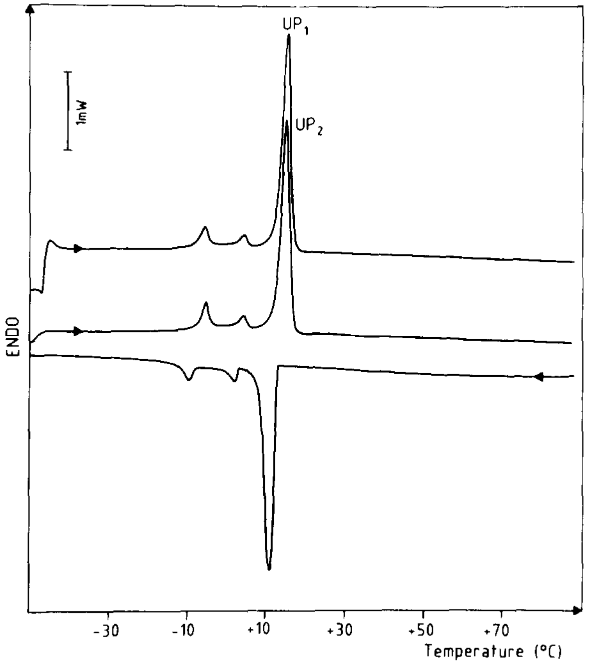

Fig. 5. DSC heating (UP$_1$), cooling (DOWN), and second heating (UP$_2$) curves of isopropyl palmitate.

thermal peaks in the heating curve, with onset temperatures of, respectively, −8.2 and 1.7°C might represent polymorphic transitions, since hydrocarbons with a long and unbranched chain can exist in several modifications (Precht et al., 1978; Junginger et al., 1979b). Fig. 5, however, shows that the thermal history of the sample did not affect these transitions, which makes the occurrence of polymorphism for IPP doubtful. Other possibilities for the DSC behaviour observed include the heterogeneity on a molecular scale of IPP or the presence of impurities having a complex phase diagram behaviour with IPP.

The third endothermal transition involving the most important enthalpy change is the melting process of IPP. The measured onset temperature of 12.3°C concurs with literature data (Elder, 1980; Weast, 1981, 1982). When cooling, IPP began to recrystallize at 12.3°C without showing supercooling. A rough estimate of the heat of fusion of IPP obtained by using the partial areas procedure yielded a value of 117 J/g.

Surfactant-water mixtures

Cetiol^R HE-water mixtures

The DSC scans obtained on heating aqueous solutions of CHE showed only one endothermal peak. For the sample containing 18% (w/w) CHE, the transition appeared with an onset temperature of 0.7°C and an area under the curve corresponding to an enthalpy change, ΔH, of 246 J/g. For the second sample containing 30% (w/w) CHE, these values are, respectively, −1.2°C and 181 J/g. The general features of this peak show that they stem from the melting of ice. In the freezing curves for the same samples, the freezing of water resulted in an exothermal peak showing an onset temperature of −11°C for the 18% (w/w) sample and −13.2°C for the sample containing 30% (w/w) CHE. The supercooling of the water below its depressed melting point prior to crystallization causes the water molecules to freeze in a short period. This results in a very sharp exothermal peak, which makes the area determination rather uncertain.

From both the melting and the freezing enthalpy values, it is apparent that part of the water present in the sample did not freeze on cooling. For poly(ethylene glycol) (PEG) and polyoxyethylene (POE) containing surfactants this is a well-known phenomenon. The non-freezable water is considered bound hydration water. Hydration results from the binding of water molecules through hydrogen bonding to the ether oxygens of the oxyethylene units. From an evaluation of the enthalpy changes caused by melting or freezing of the freezable free water at various solute levels, the hydration number of the polymer can be calculated, i.e., the number of water molecules bound per oxyethylene unit (Nelson, 1977).

Determination of the hydration number of CHE and EB3 is beyond our present scope. Bound water molecules are known to possess properties differing from the free-water phase. In dosage systems based on such hydrated surfactants, the ratio of bound to free water will affect its water release (Junginger et al., 1984) and the diffusion of drugs through the vehicle (Boddé et al., 1986) and the skin. The hydration number thus might be an important factor in the regulation of the water and drug delivery.

Eumulgin^R B3-water mixtures

In the heating scans of the EB3-water mixtures containing, respectively, 12% (w/w) and 15% (w/w) EB3, the endothermal peak caused by the melting of free-water ice also can be clearly observed. This free-water peak (P_2) was, however, preceded by a small unresolved endothermal peak (P_1), showing a maximum at −1.8°C for both samples. In the freezing curves the two peaks were fully resolved, allowing an estimation of both onset temperature and enthalpy change. The results of these measurements are summarized in Table 2. Supercooling becomes evident from the onset temperatures.

The transition giving this peak has not been identified yet. Different possibilities have been suggested.

- For PEG 5700-water systems, this transition has been ascribed to the melting of specific hydrate complexes. The presence of a trihydrate and probably also a monohydrate complex was proposed (Graham et al., 1989). From viscometric, calorimetric and melting point studies

TABLE 2

Results of DSC cooling experiments on EB3-water samples

Sample composition EB3 : H_2O (%w/w)	P_1 peak		P_2 peak	
	Onset temperature (° C)	ΔH (J/g)	Onset temperature (° C)	ΔH (J/g)
15:85	−25	−13	−14	−216
12:88	−26	−9.8	−12	−234

of POE surfactants, Heusch (1983) also suggested the existence of several strongly associated hydrates of the PEG unit.

- From DSC studies on aqueous solutions of PEG 4000, the formation of a simple binary crystalline eutectic of PEG and water has been proposed (Hager and Macrury, 1980). The existence of non-freezing water, however, makes this possibility hardly likely.
- According to other investigators this transition could show the melting/freezing of a eutectic mixture of water and hydrated polymer. This has been suggested for PEG 1550 (De Vringer et al., 1986a) as well as for POE dodecyl ethers (Andersson and Olofsson, 1987). In this case, the system might show the phase behaviour of compounds with a congruent or incongruent melting point.
- Finally, the peak might be due to the melting/freezing of a third type of water, besides free water and bound hydration water. This so-called interfacial water is believed to be water that still interacts with the polymer chain but that is not as strongly bound as bound water. It would be freezable, but it would melt and freeze at a lower temperature than free water. This corresponds to the findings of Beyer (1982) from ^2H nuclear relaxation experiments on Triton X-100/water systems.

For none of these possibilities, however, has unequivocal proof been produced.

Cetiol^R HE-Eumulgin^R B3-water mixtures

The melting and freezing curves for the samples combining both emulsifiers and water looked very much the same as the DSC scans obtained for both EB3-water samples. A typical recorder trace of a heating scan is shown in Fig. 6. Some differences could, however, be observed. The P_1 peak, appearing as a shoulder on the large free-water peak (P_2), showed its maximum at −3.8° C for the 18 : 15 : 67 sample and at −7.3° C for the 30 : 12 : 58 sample. This is markedly lower than the temperature at which the corresponding peak in the EB3-water samples showed its maximum (−1.8° C) and reflects a melting point depression effect of CHE on this transition. The general features of the P_1 peak show that its origin is the same as for the EB3-water samples.

Unlike the EB3-water system, however, P_1 could not be observed in the cooling scans of the CHE-EB3-water samples. In the low temperature regions of the heating scans (Fig. 6), the latter samples also showed two additional transitions: a very broad small endothermal transition followed by a small exothermal one. These differences point to interactions between CHE and EB3.

The P_2 transition originates from the melting/freezing of free water. In the heating curves, it appears with an onset temperature of −1.6 and −3.9° C for the 18:15:67 and the 30:12:58 sample, respectively. In the cooling curves the corresponding onset temperatures were −14.5 and −11.6° C.

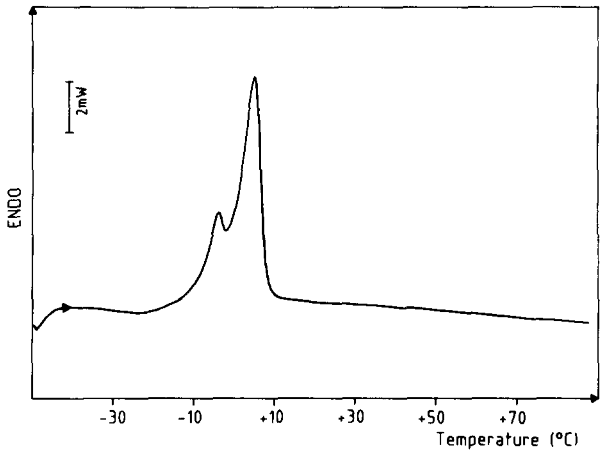

Fig. 6. DSC heating curve of a mixture containing 18% (w/w) CHE, 15% (w/w) EB3, and 67% (w/w) water.

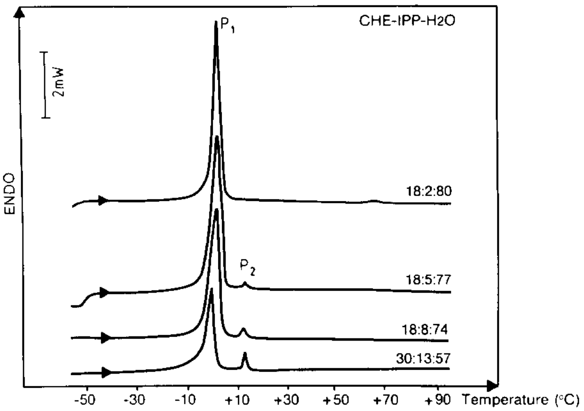

Fig. 7. DSC heating curves of mixtures containing CHE, IPP and water.

Surfactant-IPP-water mixtures

Cetiol^R HE-IPP-water mixtures

The results of DSC measurements on four different samples containing between 2 and 13% (w/w) IPP are shown in Fig. 7. Only the heating scans are given. The cooling scans showed the same pattern, although the P_2 peak was very broad and small. Macroscopically, the samples were all opalescent, whitish, unstable liquids that separated into two layers. Microscopically with polarized light, the sample containing 5% IPP appeared isotropic; in the 2% IPP sample a fine structure and in the 8% IPP sample emulsion droplets could be clearly distinguished. The 13% IPP sample, having a higher CHE content, again appeared isotropic.

In the thermograms, the transition involving the highest enthalpy change, P_1, is due to the melting of free water-ice. The parameters characterizing this peak are given on the left in Table 3. Because of the overlapping with the P_2 peak in the heating curves and the sharpness of the peak in the cooling curves, the ΔH values are only approximations. Nevertheless, it is obvious that, for samples with the same CHE content, i.e., the samples containing 2%, 5% and 8% (w/w) IPP, the onset temperatures and enthalpy changes are quite similar despite the IPP concentration, and this both in the heating and in the cooling curves. This indicates that IPP does not interfere with the hydration of this emulsifier. These ΔH values are somewhat lower than those obtained for the corresponding CHE-H_2O samples because of the lower water content of the mixtures. The sample containing 13% IPP has a higher CHE content and showed lower values for the onset temperature and for the involved enthalpy change. The former reflects a further depression of the melting point of water by the emulsifier; the latter results from the lower free water content of the sample.

The second transition observed in these thermograms at somewhat higher temperatures, P_2, is clearly associated with the addition of IPP to the CHE-H_2O samples. Appearing as a small shoulder for the 2% IPP sample, it gradually increases with the IPP content. The estimated ΔH values reported in Table 3, right-hand side, further substantiate this trend. Regardless of the IPP content of the sample, the onset temperature derived from the heating scans invariably amounted to approximately 12 °C (see Table 3). This corresponds to the temperature at which IPP, as a single component, begins to melt (see above). Thus, this

TABLE 3

Results of DSC heating (UP) and cooling (DOWN) experiments on CHE-IPP-water samples

Composition CHE : IPP : H_2O (%w/w)	Free water peak (P_1)				IPP peak (P_2)		
	Onset temperature (°C)		ΔH (J/g sample)		Onset temperature (°C)		ΔH (J/g sample)
	UP	DOWN	UP	DOWN	UP	DOWN	UP
18 : 2 : 80	0.7	−13.1	215	−179	?	−2.8	?
18 : 5 : 77	0.1	−13.1	217	−180	12.3	+0.8	3.6
18 : 8 : 74	0.1	−13.1	200	−178	12.3	+2.0	5.2
30 : 13 : 57	−1.8	−14.1	124	−117	12.2	+8.1	11.4

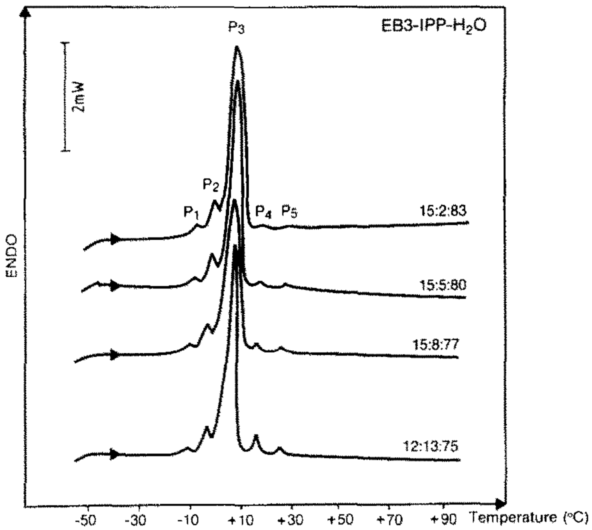

Fig. 8. DSC heating curves of mixtures containing EB3, IPP and water.

transition reflects the melting of IPP in the mixture. Unlike IPP, however, supercooling occurred on cooling. As could be expected, supercooling diminished with an increasing IPP concentration.

Eumulgin^R B3-IPP-water mixtures

The addition of IPP to the EB3-water samples resulted in a more complex DSC behaviour, as the heating scans in Fig. 8 show. In each thermogram, five overlapping endothermal heat effects could be observed. In the corresponding cooling curves, only three transitions appeared. A typical recorder trace is shown in Fig. 9. From their general features, these peaks seem to correspond to the P$_2$, P$_3$, and P$_4$ transitions in the heat flow scans. An overview of the onset temperature of the different peaks is given in Table 4. Macroscopically, the samples were all unstable, white emulsions, which separated into three layers. The polarization microscope distinguished emulsion droplets and a fine structure.

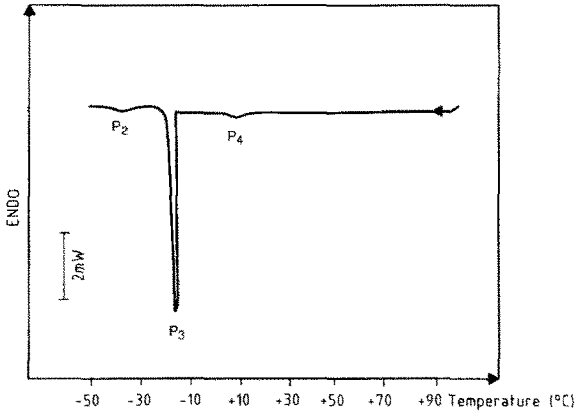

Fig. 9. DSC cooling curve of a mixture containing 15% (w/w) EB3, 8% (w/w) IPP, and 77% (w/w) water.

The P$_2$ peak, preceding the much more important free-water peak P$_3$, is comparable to the P$_1$ transition observed for the binary EB3-water mixtures. It was seen at a constant temperature of approximately $-5\,^\circ$C and exhibited marked supercooling. Because of overlapping, the enthalpy changes could only be roughly estimated and so will not be discussed in detail. In the light of further discussions, however, it is important that, for the samples with the same EB3 content, the enthalpy change accompanying this P$_2$ transition is independent of the IPP concentration. This indicates that the underlying process is not influenced

TABLE 4

Results of DSC heating and cooling experiments with EB3-IPP-water samples

Composition EB3 : IPP : H$_2$O (%w/w)	Onset temperature (°C)							
	Heating					Cooling		
	P$_1$	P$_2$	P$_3$ [a]	P$_4$ [a]	P$_5$	P$_2$	P$_3$ [a]	P$_4$ [a]
15 : 2 : 83	−11.5	−5.5	1.0	13.1	21.9	−34.4	−13.2	?
15 : 5 : 80	−12.2	−5.8	0.8	12.5	21.4	−33.1	−14.8	9.8
15 : 8 : 77	−11.3	−4.8	1.2	13.6	22.3	−32.3	−16.4	12.4
12 : 13 : 75	−12.8	−5.4	1.3	12.4	21.4	−30.8	−11.8	12.0

[a] P$_3$, free-water peak; P$_4$, IPP peak.

by IPP, whatever it might be (see above). Comparing the DSC behaviour with that of the binary EB3-water mixtures, however, shows that the presence of IPP induced the P_4 and P_5 peaks.

The P_4 peak denotes the melting of IPP in the mixtures. The size of the peak clearly increased with increasing IPP content. The cooling curves do not unequivocally establish the presence or absence of supercooling, the corresponding transitions being very broad and small. In the CHE-IPP-water mixtures, however, IPP crystallized with significant supercooling, which suggests a quite different behaviour for IPP in both emulsifier-water systems.

Another thermal feature specifically connected with the EB3-IPP-water system is the P_5 peak. As evidenced by a microscopical examination, this transition reflects the melting of a liquid crystalline structure. The low enthalpy changes accompanying this transition are in good agreement with the findings of several authors on various transitions involving liquid crystalline phases (Andersson and Olofsson, 1987; Pöllinger, 1986). The formation of this structural association requires both EB3 and IPP in addition to water.

TOW gels

TOW gels were obtained by combining the four components, CHE, EB3, IPP, and water, in specific concentration ratios. Four TOW gels each containing a different amount of IPP were selected and DSC measurements were performed. The heat flow scans are given in Fig. 10.

Comparing them with the DSC behaviour of the binary and ternary mixtures described above shows that the low temperature region of the melting curve for the TOW gel containing only 2% (w/w) IPP looks very much like the heat flow scan of the CHE-EB3-water mixtures. From the general features of the P_1 peak, one may postulate the same originating transition as for the P_1 peak in the EB3-water and the CHE-EB3-water mixtures and the P_2 peak in the EB3-IPP-water mixtures. The lower peak temperature ($-5.8°C$) as compared to the corresponding P_1 transition in the EB3-water mixture seems to be the cumulative result of the melting point depression effects caused by both CHE and IPP. The lower height of the peak in comparison with the ones measured for the corresponding EB3-water, CHE-EB3-water and EB3-IPP-water samples, however, indicates a specific intercomponent interaction underlying TOW gel formation.

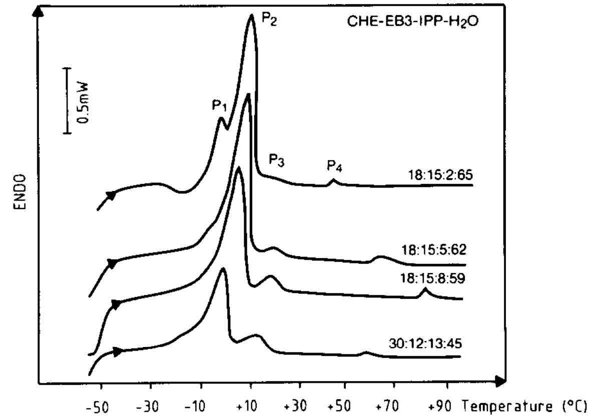

Fig. 10. DSC heating curves of TOW gels.

Another indication follows from the observation that, with increasing IPP content but constant CHE-EB3 concentrations, the thermal behaviour of the TOW gels differed more and more from that of the CHE-EB3-water mixtures (cf. Figs 6 and 10). The very broad endothermal and exothermal transitions seen at very low temperatures are no longer observed, and the P_1 transition gradually becomes less pronounced. A comparison of the latter transition with the corresponding transitions in the emulsifier-water and the emulsifier-IPP-water mixtures also shows some typical features. This transition seems to be specifically connected with the presence of EB3. For samples with the same EB3 content (as long as they were liquid) the height of the peak remained approximately constant (cf. the EB3-water and CHE-EB3-water mixtures). It was even not affected significantly by increasing IPP concentrations (cf. the EB3-IPP-water mixtures). But the moment TOW gels were formed, an increase in the IPP content caused this transition to become gradually less pronounced.

As for the binary and ternary mixtures, the transition involving the highest enthalpy change, i.e., P_2, denotes the melting of free water-ice.

Although IPP seems to act upon the behaviour of the emulsifier(s) in water to allow for the formation of TOW gels, its melting in the gels could still be observed (P_3 peak). This transition appeared as a small shoulder for the 2% IPP TOW gel that increased in size with IPP content in the same way as it did in the CHE-IPP-water and EB3-IPP-water mixtures. However, for the TOW gels the peak was clearly broader, and its broadness showed an almost twofold increase with IPP content for the TOW gels under investigation. These observations again are indicative for an interaction of IPP with one or both emulsifiers (Junginger et al., 1979a). The evolution of the broadness of the peak suggests that this interaction mainly concerns EB3. Indeed, the peak also widened with increasing IPP content in EB3-IPP-water mixtures, but it did not in the CHE-IPP-water system.

The most striking indication for the influence of IPP in the TOW gel structure, however, is given by the P_4 peak. A comparison of the onset temperature of this transition with the macroscopically determined melting point of the gels, given in Table 5, clearly shows this peak originates from the melting of the gels. For other TOW gels this gel–sol transition was confirmed by means of rheological, refractometric, and oscillatory mechanical measurements (Nürnberg and Pohler, 1984a,b). DSC/DTA measurements on various TOW gels, however, did not reveal the melting of the gels (Mubarak, 1982; Beyer and Mubarak, 1983; Jettka, 1984). This might be due to a too low sensitivity of the apparatus, or to the thermal history of the samples. Indeed, our experiments showed that this transition could be detected neither in the cooling curves nor in a second heating scan, although we did note solidification of the gel on cooling.

TABLE 5

TOW gels: comparison between the onset temperature of the P_4 transition in the DSC heat flow scans, and the melting point of the gels determined with the Ubbelohde Apparatus

Composition CHE-EB3-IPP-H_2O (%w/w)	DSC P_4 peak onset temperature (°C)	Melting point (°C)
18:15:2:65	35.5	34.7
18:15:5:62	53.8	53.8
18:15:8:59	73.0	67.4
30:12:13:45	51.6	42.5

The data in Table 5 also show that an increase in the IPP concentration involved an increase in the gel-sol transition temperature for TOW gels with the same emulsifier content. According to Eqn 1, this finding points to an increase in the structural organisation of the gel if one assumes that the entropy change does not alter significantly.

$$T_m = \frac{\Delta H}{\Delta E} \tag{1}$$

where T_m is the melting temperature of a substance, H is enthalpy, and E is entropy.

Conclusions about enthalpy changes cannot be drawn yet. Our rough estimates of these values are, however, in good agreement with literature values (Pöllinger, 1986; Nürnberg and Pohler, 1984a) and indicate that the binding forces responsible for the gel structure are probably hydrogen bonds. This was confirmed by a specific destruction of the gel structure by ureum, ions, and polyalcohols (Nürnberg and Pohler, 1984a) and by rheological measurements (Henniges, 1985). An increase in the oil content of TOW gels has been sometimes found to give rather constant ΔH values (Pöllinger, 1986). Considering Eqn 1, the resulting increase in the structural organisation of the gels should, however, also result in increasing ΔH values.

This influence of IPP concentration on the melting behaviour of TOW gels was investigated further. Quaternary CHE-EB3-IPP-water mixtures with a constant emulsifier content, i.e., 18% (w/w) CHE and 15% (w/w) EB3, but increasing IPP concentration were prepared and their melting points were determined. The results are shown in Fig. 11. As long as TOW gels were formed, i.e., for samples containing between 2 and 8% (w/w) IPP, there was an almost linear correlation between the melting point and the oil content of the gel. By further increasing the IPP content, the oil could no longer be adequately incorporated in the

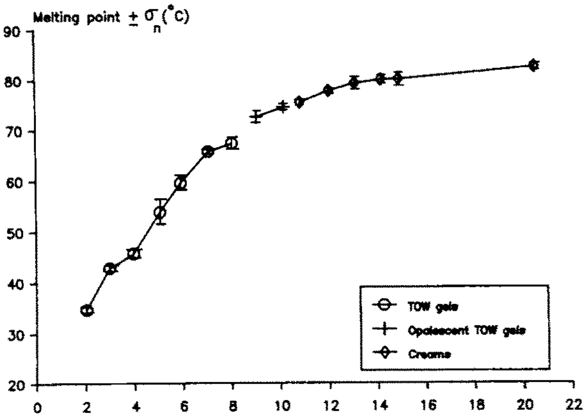

Fig. 11. The relationship between the macroscopic appearance, melting point, and IPP content of quaternary CHE-EB3-IPP-water mixtures.

emulsifier associations and formed a separate phase. At first this caused the gels to become opalescent; still higher IPP concentrations resulted in white creams. The melting point of these compositions no longer increased to the same extent with increasing IPP concentrations.

Rheological measurements showed an increase in the melting temperature of TOW gels to be accompanied by an increase in their yield value and end viscosity (Nürnberg and Pohler, 1986; Pöllinger, 1986). The melting point thus reflects the degree of structural organisation of the gel. From a combination of oscillatory mechanical and SAXD measurements, Jettka (1984) has shown that an increase in the oil content of TOW gels results in the enlargement of the emulsifier associations forming the gel structure without causing changes in the nature of these associations. Rather, the gel stiffens gradually. When still higher oil contents eventually result in the formation of opalescent gels to white creams, their oscillatory mechanical behaviour shows no further significant changes (Jettka, 1984).

Conclusions

We were able to clarify several aspects of the intercomponent interactions underlying TOW gel formation on the basis of DSC measurements on binary, ternary, and quaternary mixtures. First, we have showed that some of the water is tightly associated with both surfactants through hydrogen bonding with the hydrophilic tail. These hydrated emulsifiers interact with one another, which explains why TOW gels can only be formed in their combined presence. Although the oil component, IPP, does not interfere with the hydration of CHE, it does affect the behaviour of the emulsifiers in water, thus allowing for TOW gel formation. The interaction of IPP seems to involve mainly EB3.

Our findings as well as those from other authors allow us to conclude that the three-dimensional gel network in our TOW gels is based on hydrogen bonds linking neighbouring structural associations of hydrated emulsifier molecules. For the formation of this gel structure not only both of the emulsifiers, CHE and EB3, but also IPP seem essential. An increase in the IPP content of the TOW gels increases the number of hydrogen bonds between the emulsifier aggregates, resulting in an ever closer packing of these associations. Because of this higher structural organisation, the gel stiffens and its melting point increases. Too high IPP concentrations, however, can no longer be incorporated adequately in the emulsifier aggregates and opalescent gels or white creams are formed. The gel network basically remains the same as in the TOW gels, but the excess oil no longer induces more interactions between the structural associations. This is reflected in the further evolution of the melting point.

References

Andersson, B. and Olofsson, G., Differential scanning calorimetric study of phase changes in poly(ethylene glycol) dodecyl ether-water systems. *Colloid Polymer Sci.*, 265 (1987) 318–328.

Beyer, K., Phase structures, water binding, and molecular dynamics in liquid crystalline and frozen states of the system Triton X-100-D_2O: a deuteron and carbon NMR study. *J. Colloid Interface Sci.*, 86 (1982) 73–89.

Beyer, C. and Mubarak, K., Mikroemulsionen. *Pharmazie Zeit*, 12 (1983) 55–60.

Boddé, H.E., De Vringer, T. and Junginger, H.E., Colloidal systems for controlled drug-delivery – structure activity relationships. *Progr. Colloid Polymer Sci.*, 72 (1986) 37–42.

British Pharmacopoeia, Her Majesty's Stationery Office, London, 1988, Vol. II A, p. 93.

De Vringer, T., Joosten, J.G.H. and Junginger, H.E., A study of the hydration of polyoxyethylene at low temperatures by differential scanning calorimetry. *Colloid Polymer Sci.*, 264 (1986a) 623–630.

De Vringer, T., Joosten, J.G.H. and Junginger, H.E., A study of the gel structure in a nonionic O/W cream by differential scanning calorimetry. *Colloid Polymer Sci.*, 264 (1986b) 691–700.

Elder, R.L. (ed.), Cosmetic Ingredient Review. Final report on the safety assessment of octyl palmitate, cetyl palmitate and isopropyl palmitate. Report CIR 11-80. In: *Safety assessment of cosmetic ingredients*, Washington D.C., 1980.

Fiedler, H.P., Lexikon der Hilfsstoffe für Pharmazie, Kosmetik und angrenzende Gebiete, 3., überarb.u.erg. Aufl., Editio Cantor, Aulendorf, 1989, p. 964.

Flory, P.J., Principles of Polymer Chemistry, Cornell University Press, Ithaca, New York, 1953, p. 573.

Graham, N.B., Zulfiqar, M., Nwachuku, N.E. and Rashid, A., Interaction of poly(ethylene oxide) with solvents: 2. water-poly(ethylene glycol). *Polymer*, 30 (1989) 528–533.

Hager, S.L. and Macrury, T.B., Investigation of phase behavior and water binding in poly(alkylene oxide) solutions. *J. Appl. Polym. Sci.*, 25 (1980) 1559–1571.

Henniges, F., Untersuchungen zur Struktur und dem mechanischen Verhalten von halbfesten Zubereitungen mit *o*-Phosphorsäureestertetraethylenglykollaurylether, Dissertation, Braunschweig, 1985.

Heusch, R., Mizellare und mesomorphe Strukturen in wässrigen Polyglykoletherlösungen. *Tenside detergents*, 20 (1983) 1–12.

Jettka, W., Untersuchungen zum viskoelastischen Verhalten pharmazeutisch verwendeter halbfester Zubereitungen, Dissertation, Braunschweig, 1984.

Junginger, H., Führer, C., Ziegenmeyer, J. and Friberg, S., Strukturuntersuchungen von Salben. 2. Mitteilung: Strukturuntersuchungen an der Wasserhaltigen Hydrophilen Salbe DAB7. *J. Soc. Cosmet. Chem.*, 30 (1979a) 9–23.

Junginger, H.E., Führer, C., Beer, A. and Ziegenmeyer, J., Polymorphie bei Salben 1. Polymorphes Verhalten der Hydrophilen Salbe DAB7. *Pharm. Ind.*, 41 (1979b) 380–385.

Junginger, H., Führer, C. and Fischer, G., Structural investigations of Polyethylenglycol Ointment DAB8. In APGI, 2nd Congrès International de Technologie Pharmaceutique, Paris, 3–5 June 1980, pp. 215–221.

Junginger, H., Akkermans, A.A.M.D. and Heering, W., The ratio of interlamellarly fixed water to bulk water in O/W creams. *J. Soc. Cosmet. Chem.*, 35 (1984) 45–57.

Mubarak, K., Entwicklung und Prüfung neuer Mikroemulsionen, Dissertation, Tübingen, 1982.

Nelson, R.A., The determination of moisture transitions in cellulosic materials using differential scanning calorimetry. *J. Appl. Polym. Sci.*, 21 (1977) 645–654.

Nürnberg, E. and Pohler, W., Zur Kenntnis von 3-Komponenten-Mikroemulsionsgelen. 4. Mitteilung: der Gelcharakter optisch isotroper Tensid-H_2O-Paraffin-Systeme. *Progr. Colloid Polymer Sci.*, 69 (1984a) 64–72.

Nürnberg, E. and Pohler, W., Zur Kenntnis von transparenten 3-Komponenten-Tensidgelen. 5. Mitteilung: Schwingungsmechanische Untersuchungen. *Acta Pharm. Technol.*, 30 (1984b) 169–173.

Nürnberg, E. and Pohler, W., Zur Kenntnis von transparenten 3-Komponenten-Tensidgelen. 7. Mitt.: Stabilitätsprüfungen. *Pharm. Ind.*, 48 (1986) 1554–1556.

Pöllinger, N., Einfluss unterschiedlich ethoxylierter Derivate des Oleylalkohols sowie verschiedener Ölkomponenten auf die Ausbildung Pharmazeutisch relevanter Gele. Zur Kenntnis von Mikroemulsionsgelen, Dissertation, Erlangen, 1986.

Precht, D., Frede, E. and Greiff, R., Molekülanordnungen und Kristallgitterdefekte in Fettgemischen. *Fette, Seifen, Anstrichmittel*, 80 (1978) 344–352.

Provost, C., Transparent oil-water gels. *Int. J. Cosmet. Sci.*, 8 (1986) 233–247.

Provost, C. and Kinget, R., Transparent oil-water gels: a study of some physicochemical and biopharmaceutical characteristics. Part I. Formation of transparent oil-water gels in the 4-component-system of Eumulgin B3, Cetiol HE, isopropyl palmitate, and water. *Int. J. Pharm.*, 44 (1988a) 75–85.

Provost, C., Herbots, H. and Kinget, R., Transparent oil-water gels: study of some physico-chemical and biopharmaceutical characteristics. Part 3: Viscosity and conductivity measurements. *Pharm. Ind.*, 50 (1988b) 1190–1195.

Provost, C., Herbots, H. and Kinget, R., Transparent oil-water gels: Study of some physico-chemical and biopharmaceutical characteristics. Part IV: The in-vitro release of hydrophilic and lipophilic drugs. *Acta Pharm. Technol.*, 35 (1989a) 143–148.

Provost, C., Herbots, H. and Kinget, R., The in vitro penetration of hydrophilic and lipophilic drugs from transparent oil-water gels through excised human epidermis; a comparative study with other dermatological vehicles. *Drug Devel. Ind. Pharm.*, 15 (1989b) 25–49.

Reynolds, J.E.F., Martindale: *The Extra Pharmacopoeia*, 28th edn., The Pharmaceutical Press, London , 1982, p. 710.

Weast, R.C., *CRC Handbook of Chemistry and Physics*, 62nd edn., CRC Press Inc., Boca Raton, FL, 1981–1982, C-412.